MeV ion damage in GaAs single crystals: Strain saturation and role of nuclear and electronic collisions in defect production

Chu Ryang Wie* and T. A. Tombrello
Divisions of Physics, Mathematics, and Astronomy, California Institute of Technology, Pasadena, California 91125

T. Vreeland, Jr.
Division of Engineering and Applied Sciences, California Institute of Technology, Pasadena, California 91125
(Received 23 August 1985)

We have reported previously that the perpendicular strain produced in the surface layer (several μm thick) of GaAs(100) crystals under MeV ion irradiation saturates at $\sim 0.4\%$ regardless of the doping of the specimen, and that the parallel strain is zero within the experimental error. In this paper, the perpendicular strain in GaAs(111) and GaAs(110) crystals is reported to saturate at $\sim 0.3\%$. The ionization-induced spontaneous defect recovery is discussed in terms of the activation-energy lowering of the higher-charge-state interstitials. We suggest that inner-shell vacancies which decay by an Auger process may induce most effective self-annealing of defects created by nuclear collisions. We present an ion-lattice single-collision model which describes the production and saturation of the primary defects (interstitial, vacancy, and antisite defect) in GaAs under MeV ion or MeV electron irradiation. The model also shows that at low beam dose the concentration of interstitials and vacancies increases linearly with the product of stopping power and beam dose and is independent of the electronic stopping power. The antisite defect concentration increases initially as the square of the nuclear stopping power times the beam dose, and depends upon the electronic stopping power. The strain measured as a function of beam dose and stopping powers suggests that the strain in the room-temperature irradiated GaAs is controlled by the antisite defects.

I. INTRODUCTION

Si and Ge have been emphasized in radiation-damage studies, and the defects and their consequences in these two elemental semiconductors are quite well understood. The primary defect for these elemental crystals is a vacancy-interstitial pair. The primary defects in binary compounds are, however, more complicated. There can be two vacancies, two interstitials with two different kinds of nearest-neighbor atoms, and two antisite defects. Another difficulty in defect studies of III-V compounds is that EPR (electron paramagnetic resonance) is not able to provide clear-cut information because of nonzero nuclear spin moments of the group-III and group-V atoms.

Most radiation damage studies in GaAs involve the irradiation effects of MeV electrons,[1] neutrons,[2] and keV ions for ion implantation.[3] The collision cross section for lattice displacements is typically 10^{-23} cm^2 for MeV electrons, and 10^{-14}–10^{-12} cm^2 for keV ions. The characteristic feature of irradiation effects is the creation of isolated point defects by MeV electrons, and the creation of isolated disordered regions from collision cascades by keV ions. An electron accelerator with a beam current of ~ 1 μA/cm^2 can produce defects of 10^{-6} atomic fraction concentration in 5 h of irradiation. Thus, the study of defects using electron beams is in practice limited to $\lesssim 10^{-5}$ fractional concentration.

MeV ions can provide a range of defect concentration in between those of MeV electrons and keV ions. A MeV ion of intermediate mass (e.g., ^{12}C, ^{40}Ar) in the energy range of 1 to 25 MeV gives a collision cross section for atomic displacement of typically 10^{-17} cm^2. The energy loss per unit length in atomic displacement processes in semiconductors is on the order of the threshold atomic displacement energy per atomic spacing, i.e., a few eV/Å. Irradiation for less than an hour using a MeV ion accelerator with a particle current of ~ 100 nA/cm^2 can produce fractional defect concentrations of 10^{-6} to 10^{-2}.

Another interesting property of MeV ions in the study of radiation damage is that the ion loses most of its energy by electronic collisions. Simultaneous electronic and displacement collisions can change the charge state of defects, which will strongly affect the defect migration.[4,5] The energy loss per unit length in nuclear collisions (S_n) and in electronic collisions (S_e) is shown as a function of depth in Fig. 1 for a 15-MeV ^{35}Cl ion incident on GaAs. (The nuclear stopping power values were computed using the Kr-C formula in the paper by Wilson *et al.*,[6] and the electronic stopping power values were taken from the data table by Littmark and Ziegler[7] or that by Northcliffe and Schilling.[8])

Higher-charge-state interstitials in Ge tend to annihilate with vacancies[5] at lower temperatures. The 65-K defect with an activation energy of ~ 0.15 eV (Ref. 9) in electron-irradiated Ge was reported to anneal with a migration energy of 0.004 eV for interstitials whose charge state altered under 0.5 MeV electron irradiation, which induces annealing.[10] Radiation-enhanced annealing with low-energy electrons has been observed for Si, Ge, and GaAs.[1,11,12] The doses necessary to bring the radiation annealing to completion were about 3 orders of magnitude larger for Si and Ge than for GaAs.

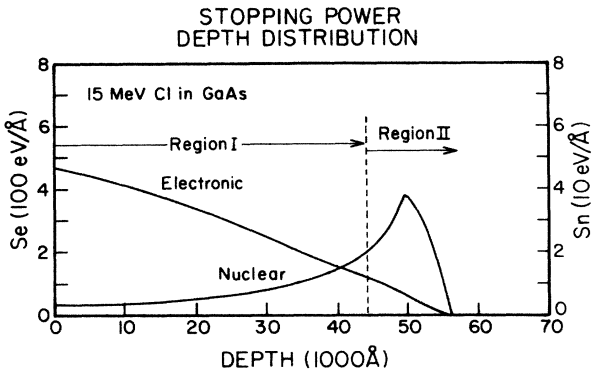

FIG. 1. Depth distribution of the stopping power for a 15-MeV Cl ion incident on GaAs. The curves were obtained by a Gaussian convolution, with the half-width equal to the range straggling, of the stopping power distribution from the Kr-C formula (Ref. 6) and from Northcliffe and Schilling (Ref. 8).

In this paper, we report the MeV ion damage in GaAs single crystals. The strain induced by the radiation damage is shown to saturate and to be partially annealed by the ionization process. The experimental results are presented in Sec. II, and an ion-lattice collision model is presented in Sec. III.

II. EXPERIMENTALS AND RESULTS

GaAs(100), GaAs(111), and GaAs(110) single-crystal surfaces were bombarded at room temperature with Cl, O, and C ions in the energy range between 3 and 15 MeV. Among the GaAs crystals with various dopants (Cr, Si, Zn, or Te), the Cr-doped semi-insulating crystals had the best crystal quality as checked before beam irradiation by x-ray rocking-curve measurement, which showed the smallest x-ray broadening for these crystals. Thus, the Cr-doped crystals were used in most measurements. MeV

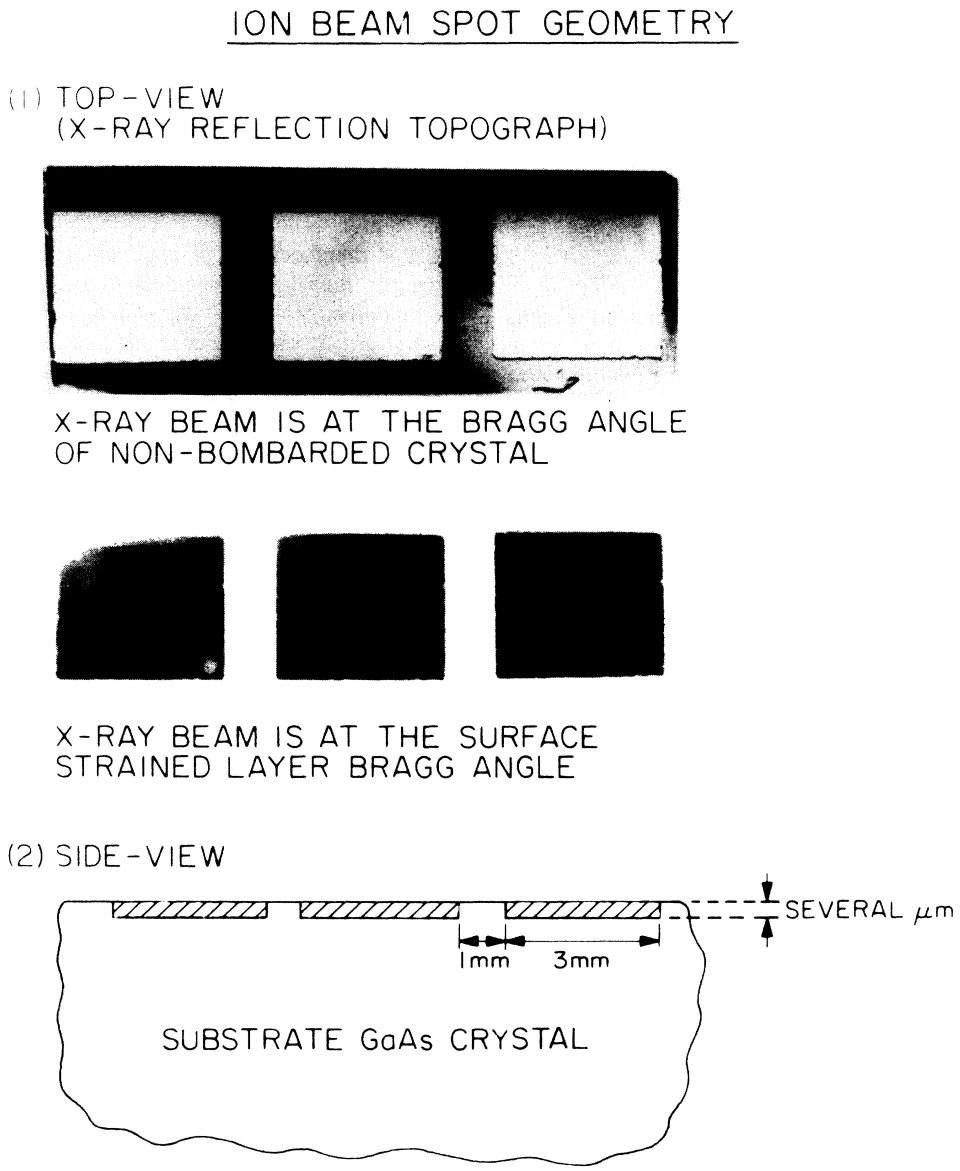

FIG. 2. Ion beam spot geometry in GaAs. The spot size is about 3×3 mm^2. Black corresponds to high-reflection intensity.

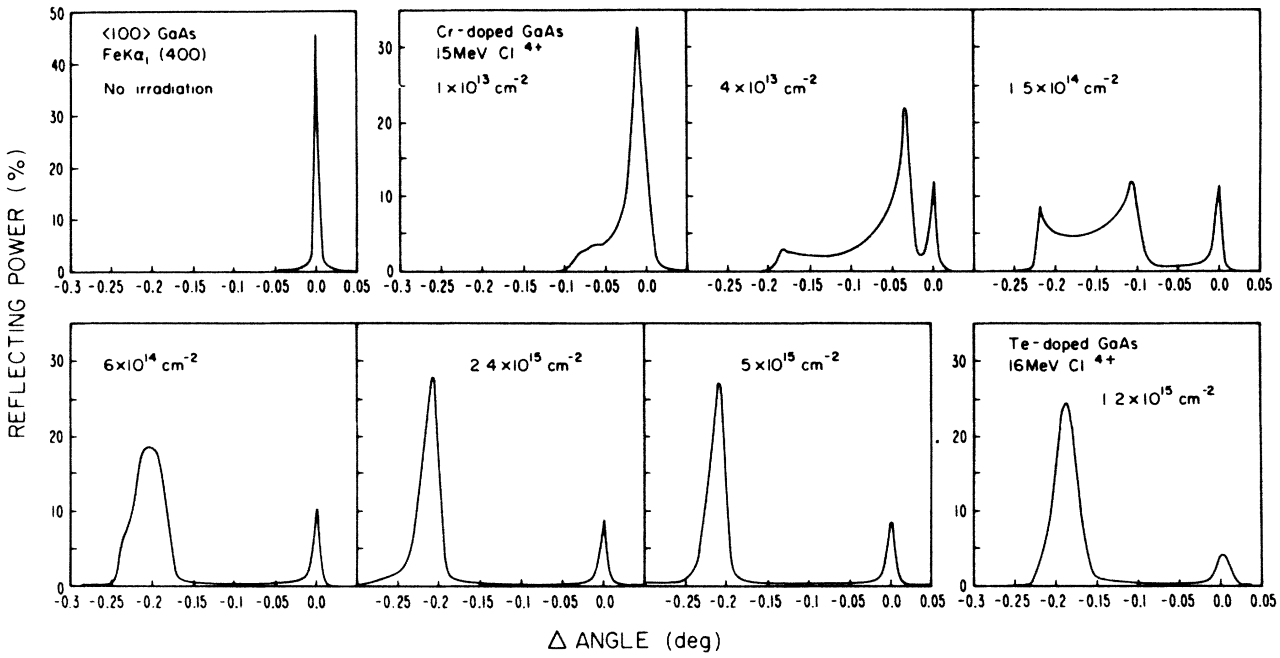

FIG. 3. X-ray rocking curves for 15-MeV Cl-ion-bombarded GaAs(100) crystals. The reflection power is recorded at each angle for a (400) symmetric reflection of Fe $K\alpha_1$ radiation. The small peak at zero angle is from the undamaged substrate crystal beyond the ion range.

ion irradiation was performed at room temperature using the tandem Van de Graaff accelerator at the California Institute of Technology with bombardment doses ranging from 10^{13} to 5×10^{15} ions/cm^2.

The geometry of irradiated beam spots on GaAs samples is shown in Fig. 2. The x-ray reflection topographs, taken with Fe $K\alpha_1$ radiation at the Bragg angle of the virgin crystal (top) or of the strained surface layer (second) for symmetric reflection, visibly demonstrate the different lattice spacing along the surface normal of the bombarded region from that of the unbombarded region. The x-ray rocking curve was obtained from the irradiated regions of (100), (111), and (110) GaAs crystals. The experimental technique is described in our earlier paper.[13,14]

Rocking curves taken at room temperature from 15-MeV Cl-ion-bombarded GaAs(100) crystals are shown in Fig. 3. The symmetric (400) reflection of Fe $K\alpha_1$ radiation was recorded at each step angle (varying by 0.0015°) for each ion beam dose. The symmetric reflection measures the strain perpendicular to the sample surface. The most prominent feature of Fig. 3 is the development of a relatively sharp symmetric peak at around $-0.22°$ after a high-dose ($D > 10^{15}$ ions/cm^2) irradiation, which indicates that the perpendicular strain saturates to about 0.4% for GaAs(100) and that the strained surface layer acquires a relatively small lattice disturbance from the MeV ion radiation damage. In a separate paper,[15] we show that low-temperature recovery stage defects such as close Frenkel pairs, divacancies, or interstitials produce major lattice distortion in III-V compounds. The small x-ray broadening indicates that the majority of defects in the irradiated surface layer are substitutional defects, and we show in Sec. III that those defects are most likely antisite defects and antisite defect complexes.

The saturation perpendicular strain for GaAs(111) and GaAs(110) crystals was $\sim0.3\%$ for both cases. The parallel strain, obtained by 422, 511, and 333 asymmetric reflections for GaAs(100) crystals, was shown to be very small [i.e., $(0\pm0.15)\%$] in our earlier paper[13] and in the thesis by Wie.[16] Recently, the Raman spectroscopy measurement of optical-phonon frequency shifts of the LO mode for GaAs(100), the TO mode for GaAs(110), and the LO and the TO modes for GaAs(111) has confirmed[17] our observation of the negligible parallel strain in the surface layer.

A dynamical x-ray-diffraction theory was applied to the analysis of x-ray rocking curves.[18] A model was developed to calculate x-ray rocking curves for a crystalline film for given structure factor, film thickness, and strain. The analysis provides strain and damage depth distributions in the layer approximation by fitting the calculated rocking curve to the experimental curve. For more details in theory and analysis the readers are referred to our separate paper[18] or to the thesis by Wie.[16]

Figure 4 shows the depth distribution of perpendicular strain at each beam dose in 15-MeV Cl-ion-bombarded GaAs(100) crystals. This distribution was obtained by drawing a smooth curve through the steplike distribution of strain in the layer approximation.[16,18] The figure shows explicitly the strain depth distribution at each beam dose and the strain saturation in the surface layers after a high-dose bombardment. The saturation of antisite defects, which are proposed as being responsible for the strain in room-temperature irradiated GaAs crystals, is explained by an ion-lattice single-collision model in Sec. III, incorporating interstitials as the transient defects pro-

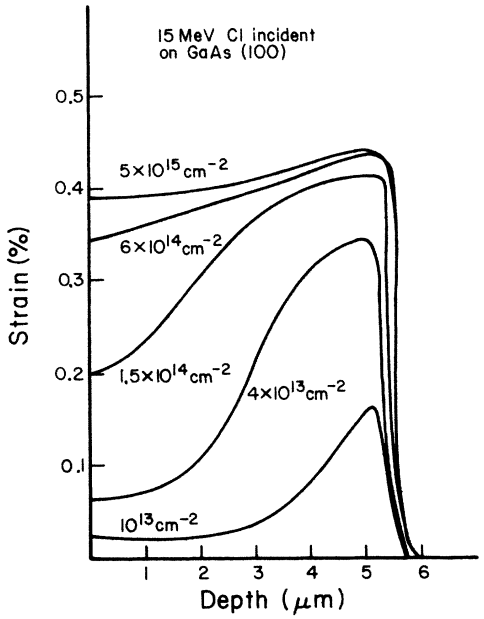

FIG. 4. Depth distribution of perpendicular strain in GaAs(100) bombarded with 15-MeV Cl ions. A detailed analysis to obtain the distribution from the rocking curves in Fig. 3 is given in Ref. 15.

duced by nuclear collisions.

The perpendicular strain at the sample surface was obtained from the depth profiles, and is plotted in Fig. 5 as a function of ion beam dose. The beam dose is renormalized to a functional form of $(1+kS_e)DS_n$, where D is the ion beam dose, S_e is the electronic stopping power, and S_n is the nuclear stopping power of the ion at the sample surface (see Sec. III). Figure 6 shows that the data curves fit for $k=-0.09$ and appropriate units are given in the figure. The mismatch in the data curves for ions differing in mass by approximately a factor of 2 may be due partially to the uncertainty in the relative stopping-power values. This result demonstrates that the damage produced by nuclear collisions is partially annealed by electronic ionization.

Table I lists the radius of maximum charge density of various wave functions of Ga and As with corresponding ionization energy,[19] and the atomic displacement cross section (for a 10-eV displacement energy) and corresponding impact parameter for 15-MeV Cl and 4-MeV O ions in GaAs. The impact parameter for atomic displacement is seen to be comparable to the radii of M-shell electrons. Thus, it can be argued that a significant fraction of the interstitial atoms displaced by nuclear collisions may well have M-shell vacancies.

In a paper by Palmer various suggested ionization effects were discussed in the production, migration, and annealing of irradiation-induced lattice defects in semiconductors.[20] It was discussed in that paper that the migration behavior of defects subsequent to their production is strongly influenced by charge-state effects and macroscopic ionization densities, and local energy release due to electron-hole recombination at defects can have very significant effects. This latter process is effective for many defects in GaAs and GaP, and for at least certain defects at low temperature in Si.

Auger decay of an M-shell vacancy in a displacing interstitial atom, which is likely to be at 1+ or 2+ charge state from the valence holes, will result in an additional 2+ charge, which will lead to a 3+ or 4+ final charge state for the displacing atoms. Also, the Auger decay of an M-shell vacancy in Ga or As will release ~ 100 eV through the Auger electrons, which may produce additional electronic holes in the atoms surrounding the displacing interstitial atom.

Considering the earlier reports that higher-charge-state interstitials in Ge migrate with lower activation energies,[9] and that ionization-induced recovery occurs in GaAs with

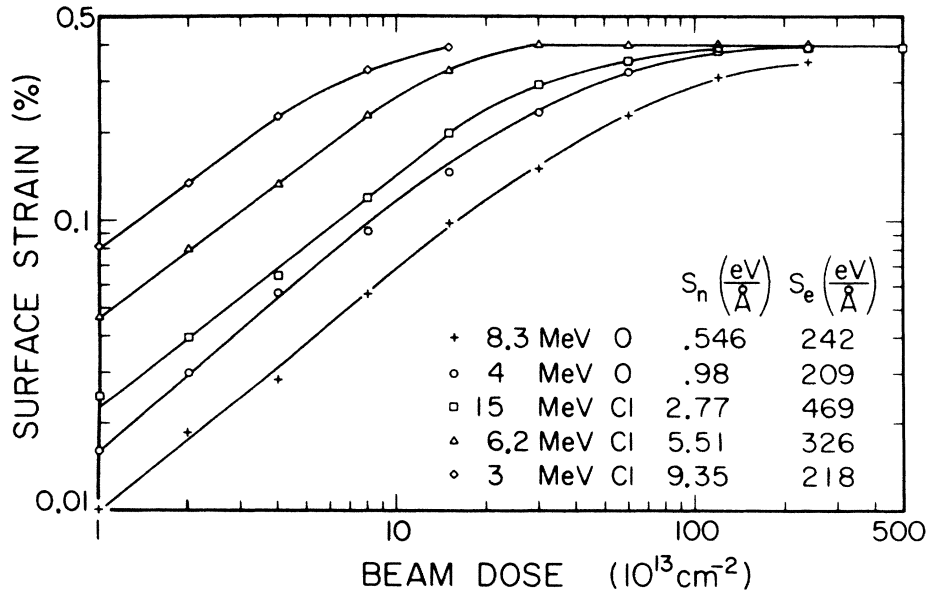

FIG. 5. Perpendicular strain at the GaAs(100) surface plotted versus beam dose for various bombarding ions.

TABLE I. Radius and binding energy of electron at various atomic levels in Ga and As, from Slater (Ref. 19). (b) Rutherford collision cross section and corresponding impact parameter for lattice displacement in GaAs (10-eV displacement threshold).

(a)

Electron shell	Radius at maximum charge density (Å)		Binding energy (Ry)	
	Ga	As	Ga	As
$1s$	0.017	0.016	764	875
$2s$	0.103	0.097	96.4	113
$2p$	0.078	0.073	83	99
$3s$	0.31	0.29	11.8	15.4
$3p$	0.31	0.29	7.9	10.8
$3d$	0.28	0.25	1.6	3.4
$4s$	0.92	0.84	0.93	1.30
$4p$	1.13	1.01	0.44	0.68

(b)

	Cross section (10^{-16} cm^2)	Impact parameter (Å)
15-MeV ^{35}Cl	0.64	0.45
4-MeV ^{16}O	0.24	0.28

higher efficiency than in Ge,[1] it is suggested that the M-shell vacancies in displacing Ga or As interstitial atoms give rise to most effective self-annealing in MeV-ion-bombarded GaAs.

In Sec. III we present an atomistic model for the point-defect production and saturation in GaAs crystals by MeV ion irradiation. The dependence of defect concentration in the low-dose limit on the electronic stopping power suggests that the strain in room-temperature irradiated GaAs is most likely controlled by the antisite defects.

III. AN ION-LATTICE SINGLE-COLLISION MODEL

In this section we present a model for the production and saturation of point defects in GaAs by an ion-lattice single-collision process. This model predicts that the point defects (vacancies, interstitials, and antisite defects) in GaAs saturate after a high-beam dose if the defects are produced by a single-collision process (i.e., no collision cascades) as in the case of MeV electrons and MeV ions.

By nuclear displacement collisions, atoms in correct lattice sites (N_c) in antisites (N_A), or in interstitial sites (N_I) are displaced into transient interstitial sites, from which they can migrate into correct lattice sites with probability α, or into antisites with probability β, or remain in the interstitial sites with probability $1-\alpha-\beta$.

For a given mass and energy the cross section for lattice displacements depends upon the target mass, atomic number, and binding energy, which are close for Ga and As in GaAs. We shall thus assume that the displacement cross sections (σ) for the correct sites and antisites are the same in GaAs, but different from the cross section (σ') for interstitial atoms, which may have much less binding energy.

Thus, the basic processes can be depicted as

$$\begin{aligned} &N_C \underset{\alpha}{\overset{\sigma}{\rightleftarrows}} N_I \xrightarrow{\beta} N_A , \\ &N_A \underset{\beta}{\overset{\sigma}{\rightleftarrows}} N_I \xrightarrow{\alpha} N_C , \\ &N_I \xrightarrow{\sigma'} N_I \begin{cases} \xrightarrow{\alpha} N_C \\ \xrightarrow{\beta} N_A \end{cases} . \end{aligned} \tag{1}$$

The probabilities of interstitial migration into correct sites (α) or into antisites (β) will be proportional to the number of open lattice sites (i.e., vacancies) which equals the number of interstitials. Therefore,

$$\begin{aligned} \alpha &= \alpha_0 \frac{N_0 - N_c - N_A}{N_0} , \\ \beta &= \beta_0 \frac{N_0 - N_c - N_A}{N_0} , \end{aligned} \tag{2}$$

where N_0 is the total number of atoms in the crystal.

Let $y = N_c/N_0$, $z = N_A/N_0$, and t equals the ion beam dose (D). Then, the equation for the collision displacements and interstitial migration processes depicted in (1) will be

$$\begin{aligned} \frac{dy}{dt} &= -\sigma y(1-\alpha) + \sigma z\alpha + \sigma'(1-y-z)\alpha , \\ \frac{dz}{dt} &= -\sigma z(1-\beta) + \sigma y\beta + \sigma'(1-y-z)\beta . \end{aligned} \tag{3}$$

Equations (2) and (3) lead to

$$\begin{aligned} \frac{dy}{dt} &= -\sigma y + \alpha_0\sigma(y+z)(1-y-z) + \alpha_0\sigma'(1-y-z)^2 , \\ \frac{dz}{dt} &= -\sigma z + \beta_0\sigma(y+z)(1-y-z) + \beta_0\sigma'(1-y-z)^2 . \end{aligned} \tag{4}$$

The electronic ionization will affect the probabilities α_0 and β_0. Even though σ' is larger than σ, the solution of Eqs. (4) shows that the behavior of antisite defect concentration (z) and interstitial concentration ($1-y-z$) is exactly the same in the low-dose limit for both $\sigma' \neq \sigma$ and $\sigma' = \sigma$. Thus, we give the solutions for Eqs. (4) for the case of $\sigma' = \sigma$, with initial conditions of $y = 1$ and $z = 0$ at $t = 0$,

$$\frac{y}{\alpha_0} - \frac{z}{\beta_0} = \frac{1}{\alpha_0} e^{-\sigma t}$$

and

$$y + z = 1 - \frac{1}{1+\alpha_0+\beta_0}(1 - e^{-\sigma(1+\alpha_0+\beta_0)t}) . \tag{5}$$

In the low-dose limit,

$$z \simeq \tfrac{1}{2}\beta_0(\sigma t)^2 \text{ and } 1 - z - y \simeq \sigma t . \tag{6}$$

Since the electronic ionization will change the probability β_0 and α_0, we expand β_0 in power series in the electronic stopping power (S_e),

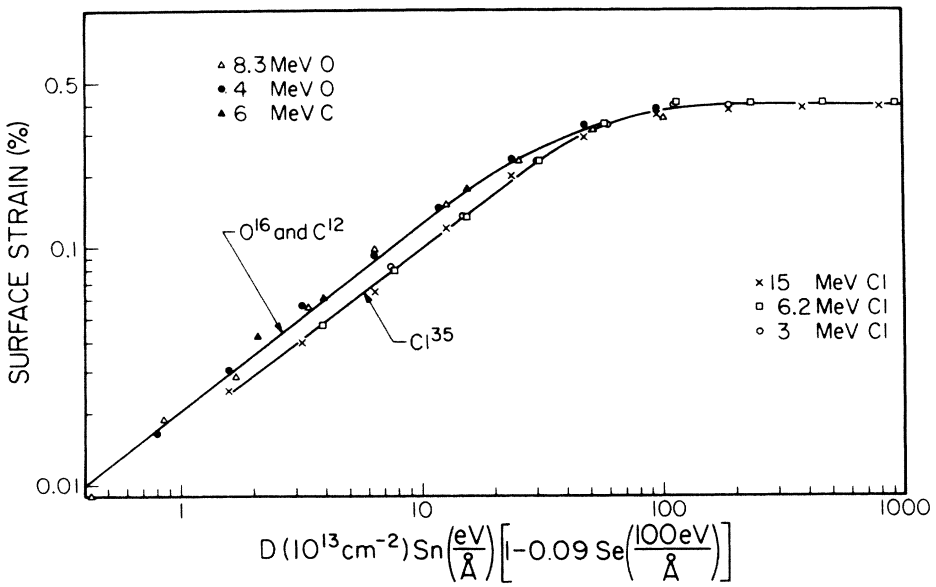

FIG. 6. Abscissa in Fig. 5 is renormalized to the form $DSn(1+kSE)$. The ionization-induced strain recovery is demonstrated in this plot by the negative sign of k. Note that the expression on the abscissa is proportional to $(N_A)^{1/2}$. The two straight lines in the plot correspond to a surface strain that is proportional to $N_A^{0.39}$.

$$\beta_0 \simeq \beta_0' + \beta_0'' S_e \ . \tag{7}$$

Therefore, in the low-dose limit,

$$\begin{aligned} &N_A \equiv \text{antisite defect concentration} \\ &\quad \text{is proportional to } \left[1+\frac{\beta_0''}{\beta_0'}S_e\right](DS_n)^2 \ . \\ &N_I \equiv \text{interstitial concentration} \\ &\quad \text{is proportional to } DS_n \ , \end{aligned} \tag{8}$$

and the vacancy concentration is the same as the interstitial concentration.

In the high-dose limit, Eqs. (5) result in the saturation concentration of

$$\begin{aligned} &\text{antisite defects} = \frac{\beta_0}{1+\alpha_0+\beta_0} \ , \\ &\text{interstitials} = \text{vacancies} = \frac{1}{1+\alpha_0+\beta_0} \ . \end{aligned} \tag{9}$$

The solution for $\sigma' \neq \sigma$ results in the saturation concentration of

$$\begin{aligned} &\text{antisite defects} = \frac{\beta_0}{\alpha_0+\beta_0}\frac{[(2\sigma'-\sigma)(\alpha_0+\beta_0)+1]-\{[(2\sigma'-\sigma)(\alpha_0+\beta_0)+\sigma]^2-4\sigma'(\sigma'-\sigma)(\alpha_0+\beta_0)^2\}^{1/2}}{2(\sigma'-\sigma)(\alpha_0+\beta_0)} \ , \\ &\text{interstitials} = \frac{[\sigma^2+(1+\alpha_0+\beta_0)^2+4(\sigma'-\sigma)\sigma(\alpha_0+\beta_0)]^{1/2}-\sigma(1+\alpha_0+\beta_0)}{2(\sigma'-\sigma)(\alpha_0+\beta_0)} \ . \end{aligned} \tag{10}$$

Equation (8) and Fig. 6 suggest that the strain in room-temperature irradiated GaAs is controlled by antisite defects with little effect from interstitials or vacancies. If the surface strain is proportional to z^n, then $n \simeq 0.39$ and $\beta_0''/\beta_0' \simeq -0.18$ Å/(100 eV) from Eq. (8) and Fig. 6.

As discussed in our separate paper,[16] the point defects, i.e., interstitials, vacancies, and antisite defects, in room-temperature irradiated GaP(100) single crystals all saturate. We thus suggest that a similar model holds for GaP and other binary compound semiconductors with suitable modifications of the displacement cross sections and the interstitial migration probabilities.

ACKNOWLEDGMENTS

This work was supported in part by the National Science Foundation (under Grant No. DMR-83-18274), by Schlumberger-Doll Research, by the Caltech President's Fund, and by the Alexander von Humboldt Foundation (Bonn, Germany).

*Permanent address: Department of Electrical and Computer Engineering, State University of New York at Buffalo, Amherst, N.Y. 14260.

[1]K. Thommen, Radiat. Eff. **2**, 201 (1970).

[2]K. V. Vaidyanathan and L. A. K. Watt, in *Radiation Effects in Semiconductors,* edited by J. W. Corbett and G. D. Watkins (Gordon and Breach, New York, 1971), p. 293.

[3]S. T. Picraux, Radiat. Eff. **17**, 261 (1973).

[4]M. Y. Fan, in *Radiation Effects in Semiconductors,* Ref. 2, p. 411.

[5]J. W. McKay and E. E. Klontz, in *Radiation Effects in Semiconductors,* Ref. 2. p. 41.

[6]W. D. Wilson, L. G. Haggmark, and J. P. Biersack, Phys. Rev. B **15**, 2458 (1977).

[7]U. Littmark and J. F. Ziegler, *Handbook of Range Distributions for Energetic Ions in All Elements* (Pergamon, New York, 1980), Vol. 6.

[8]L. C. Northcliffe and R. F. Schilling, *Nuclear Data Tables* (Academic, New York, 1970), Nos. 3 and 4.

[9]J. Zizine, in *Radiation Effects in Semiconductors,* edited by F. L. Vook (Plenum, New York, 1968), p. 186.

[10]W. D. Hyatt and J. S. Koehler, in *Radiation Effects in Semiconductors,* Ref. 2, p. 59.

[11]J. W. McKay, E. E. Klontz, and G. W. Goveli, Phys. Rev. Lett. **2**, 164 (1959).

[12]L. L. Sivo and E. E. Klontz, Phys. Rev. **178**, 1264 (1968).

[13]C. R. Wie, T. Vreeland, Jr., and T. A. Tombrello, Mater. Res. Soc. Symp. Proc. **35**, 305 (1985).

[14]C. R. Wie, T. Vreeland, Jr., and T. A. Tombrello, Nucl. Instrum. Methods B **9**, 25 (1985).

[15]C. R. Wie, T. Vreeland, Jr., and T. A. Tombrello, Nucl. Instrum. Methods B (to be published).

[16]C. R. Wie, Ph.D. thesis, California Institute of Technology, 1985.

[17]G. Burns (private communication).

[18]C. R. Wie, T. Vreeland, Jr., and T. A. Tombrello, J. Appl. Phys. (to be published).

[19]J. C. Slater, *Quantum Theory of Atomic Structure* (McGraw-Hill, New York, 1960), Vol. I, pp. 206 and 210.

[20]D. W. Palmer, in *International Conference on Radiation Effects in Semiconductors,* Dubrovnik, Yugoslavia, 6–9 Sept. 1976, edited by L. F. Eastman (IOP, Bristol, 1977), p. 144.

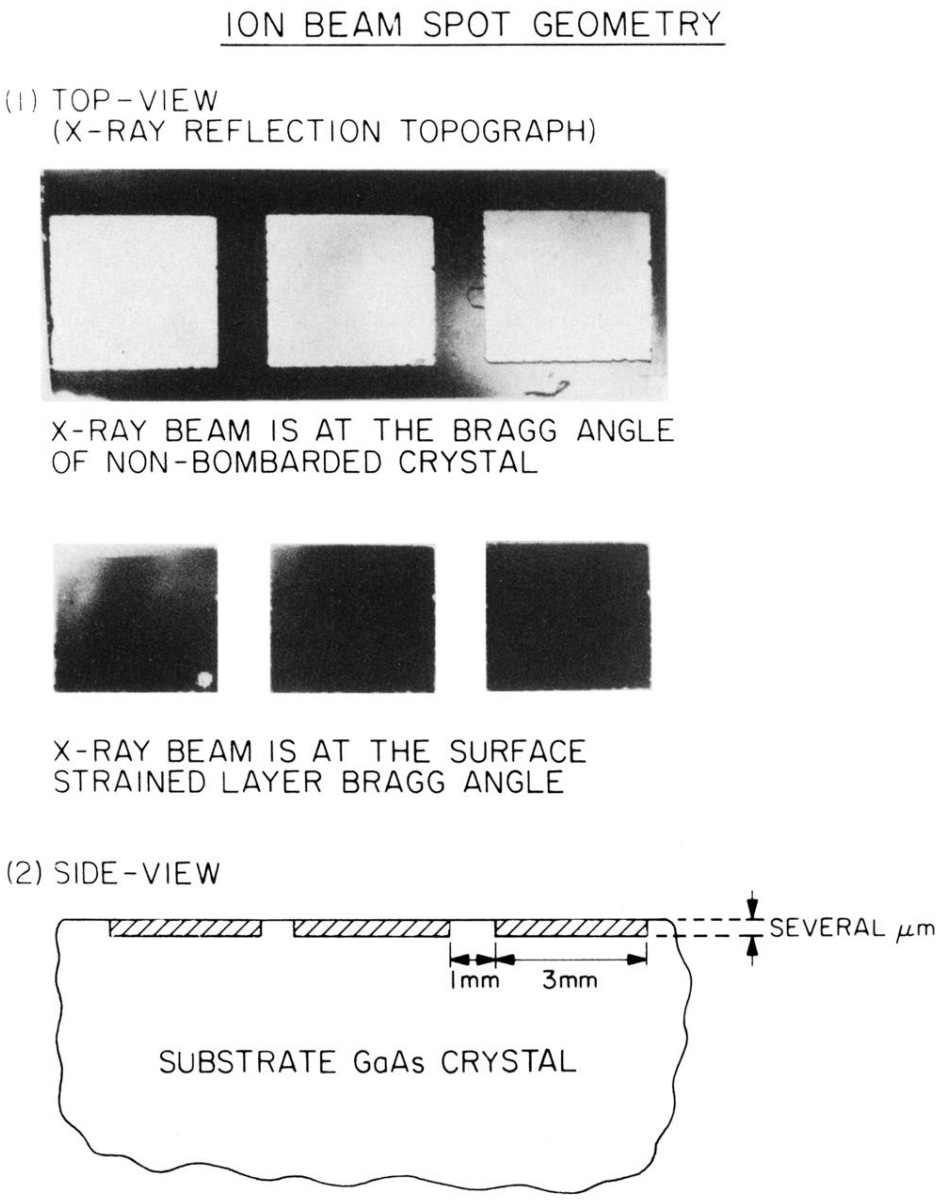

FIG. 2. Ion beam spot geometry in GaAs. The spot size is about 3×3 mm^2. Black corresponds to high-reflection intensity.